ON THE THERMOELASTIC RESPONSE OF A GRADIENT ELASTIC HALF-SPACE SUBJECTED TO THERMAL SHOCK ON THE BOUNDARY

Theodosios K. Papathanasiou[1], Panos A. Gourgiotis[1], Francesco DalCorso[1] and Thanasis Zisis[2]

[1]DICAM, University of Trento
Trento, I-38123, Italy
e-mail: t.papathanasiou@unitn.it; web page: http://www.ing.unitn.it/~dalcorsf/

[2]Department of Mechanics
National Technical University of Athens
Athens, 15780, Greece

Keywords: Gradient elasticity, Thermal stresses, Refractories, Galerkin finite elements.

Abstract. *The thermoelastic problem of a half-space subjected to thermal shock on its boundary is analysed for the case when the bulk is a microstructured solid, within the framework of the strain gradient theory of elasticity. Heat exchange through convection with a surrounding fluid, whose temperature suddenly increases by a specific amount, is imposed uniformly on the traction free surface of the half-space as a Robin type boundary condition for the temperature field. Both the weakly coupled problem of thermal stresses and the fully coupled thermoelastic response are studied. Classical Fourier heat transfer is assumed. The standard Galerkin finite element method is employed for the solution of the corresponding initial-boundary value problem which, due to the spatially uniform temperature of the free surface, is rendered one dimensional. Special finite elements are developed featuring quadratic Lagrange shape functions for the approximation of the temperature and Hermite polynomials of 5th degree for the discretization of the displacement field. The dispersive nature of the generated pulses that propagate inside the half space, characteristic for the gradient elasticity equations and absent in the classical theory, is demonstrated through a series of numerical experiments, while the effect of the microinertia and strain gradient parameters is studied*

1 INTRODUCTION

Severe thermal shock represents the main loading service condition for many applications, such as the analysis of refractories employed in liquid steel technology. A detailed description of these phenomena is fundamental for the advanced design of refractory devices towards the improvement of safety conditions of the metal flow processes. The thermoelastic problem of a half-space subjected to thermal shock on its boundary is here considered and solved for the case when the bulk is a microstructured solid, within the framework of the strain gradient theory of elasticity [1]. The same problem regarding classical elastic materials has been treated by many authors [2], [3], [4] and has aroused considerable interest [5], [6].

Heat exchange through convection with a surrounding fluid, whose temperature suddenly increases by a specific amount, is imposed uniformly on the traction free surface of the half-space (see Fig. 1) as a Robin type boundary condition for the temperature field. Both the weakly coupled problem of thermal stresses and the fully coupled thermoelastic response are studied. Classical Fourier heat transfer is assumed. The governing equations have already been presented by several authors [4], [7], [8], [9], [10] as a special case of more general thermoelastic models for materials with micro-structure.

The standard Galerkin finite element method is employed for the solution of the corresponding initial-boundary value problem which, due to the spatially uniform temperature of the free surface, is rendered one dimensional. Special finite elements are developed featuring quadratic Lagrange shape functions for the approximation of the temperature and Hermite polynomials of 5th degree for the discretization of the displacement field. The vertical method of lines is employed and the resulting second order Ordinary Differential Equation system is transformed into a first order one and integrated with the use of an Implicit Runge Kutta procedure. Validation of the numerical approximation is performed through the successful representation of an energy balance criterion derived for the weak solution, as the number of elements and time increments increases. The dispersive nature of the generated pulses that propagate inside the half space, characteristic for the gradient elasticity equations and absent in the classical theory, is demonstrated through a series of numerical experiments, while the effect of the microinertia and strain gradient parameters is studied. The aforementioned thermoelastic system and solution procedure are intended to serve as high accuracy simulation modules for the analysis and

design of refractories, ceramic thermal barrier coatings and functionally graded layers, where the underlying microstructure (grains) of the employed materials is a significant parameter.

The paper is organized as follows: Initially, the governing equations are presented along with appropriate boundary and initial conditions and the respective Initial-Boundary Value Problem (IBVP) is set in the strong form. Subsequently, after the introduction of suiting nondimensional quantites, the IBVP is reformulated in nondimensional form. Section 3 is devoted to the derivation of a variational formulation for the same problem based on which, the finite element solution procedure will be attained. In addition, the stability of the weak solution is proved. The special thermoelastic elements developed are the subject of section 4. Finally, several examples regarding to the thermoelstic response solution of the problem under consideration and numerical experiments demonstrating the robustness of the proposed finite element scheme are presented in section 5.

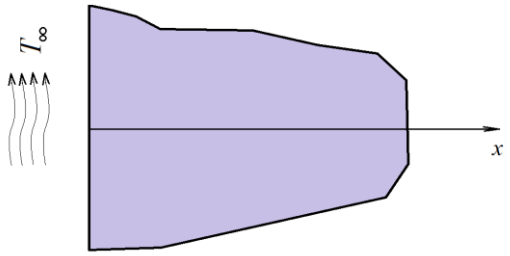

Figure 1. Gradient elastic half-space subjected to thermal shock through convective heat transfer on the boundary.

2 GOVERNING EQUATIONS AND NONDIMENSINAL QUANTITIES

2.1 Governing Equations

In the following we consider a homogeneous gradient elastic half space. The half-space is assumed to be initially at uniform temperature T_o and the upper surface is suddenly subjected to convection heat transfer with a surrounding fluid of temperature $T_\infty > T_o$ at time instant $t = 0$ and for all $t > 0$. Let $\bar{J} \in \mathbb{R}_+$ and set $Q \doteq (0,\infty)\times(0,\bar{J})$. The governing equations for the thermoelastic response of the half-space, have been derived in the framework of gradient elasticity theory as a special case of more general thermoelastic models [9], [10]. Introducing the displacement field $(u,v,w) = (u,0,0)$ and the temperature difference (with respect to the reference state T_o) $\theta = T - T_o$ these equations, if classical Fourier heat transfer is assumed, are

$$\rho c_e \theta_t - k\theta_{xx} + T_o a(3\lambda + 2\mu)u_{xt} = 0 \quad \text{, in } Q \text{ and} \tag{1}$$

$$\rho u_{tt} - 3^{-1}\rho H^2 u_{xxtt} - (\lambda + 2\mu)\left(u - g^2 u_{xx}\right)_{xx} + a(3\lambda + 2\mu)\theta_x = 0 \text{, in } Q \tag{2}$$

where ρ, c_e, k, a are the material density, specific heat capacity under constant strain, thermal conductivity and thermal expansion coefficient respectively. The classical notation λ, μ is used for the Lamé constants of elasticity. Finally, the characteristic lengths associated with gradient elasticity are H and g. On the surface of the half-space, zero traction conditions are imposed, expressed as [1]

$$u_{xx} = 0 \text{ and } 3^{-1}\rho H^2 u_{xtt} + (\lambda + 2\mu)(u_x - g^2 u_{xxx}) - a(3\lambda + 2\mu)\theta = 0,\ x = 0. \tag{3}$$

The convection heat transfer occurring at $x = 0$ is expressed through Newton's law of cooling as

$$k\theta_x = C_c\left(\theta - \theta_\infty\right), \text{ where } \theta_\infty = T - T_\infty. \tag{4}$$

The surrounding fluid medium temperature is assume to be a function of the temporal variable with the form

$$T_\infty(t) = T_o + \Phi f(t), \tag{5}$$

where Φ is the temperature increase, with respect to the reference state, attained by the surrounding medium and $f(t):[0,\bar{J}]\to[0,1]$ is a function characterizing the temperature forcing variation with respect to time. For the classical 'thermal shock' forcing it is $f(t)=H(t-t_0)$, where H denotes the Heaviside function. Mollified versions of thermal shock conditions may be also modeled by selecting appropriately the form of f (e.g. ramp functions) as shown in Figure 2.

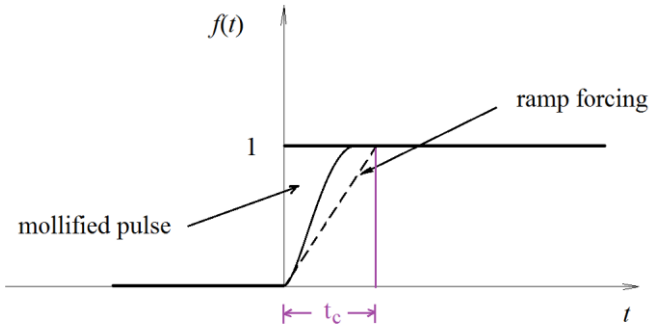

Figure 2. Surrounding medium temperature time profile.

For $x\to\infty$ zero displacement, displacement gradient and temperature are assumed. The above system is supplemented by zero initial conditions expressed as

$$u(x,t=0)=u_t(x,t=0)=\theta(x,t=0)=0\,. \tag{6}$$

In the following subsection, suitable nodimensional quantities are introduced so as to establish the proper length and time scales for the study of the phenomenon of thermoelastic pulse propagation.

2.2 Nondimensional Form

Let us introduce the thermal diffusivity $\kappa=k/(\rho c_e)$ and elastic P-wave speed $c_{PW}=\sqrt{(\lambda+2\mu)/\rho}$. The characteristic length of classical thermoelasticity is $\varepsilon=\kappa/c_{PW}$. Utilizing these parameters, the following nondimensional quantities are defined

$$\xi=x/\varepsilon\ ,\ \eta=c_{PW}t/\varepsilon\ ,\ \Theta=\theta/T_o\ ,\ U=u/\varepsilon\,. \tag{7}$$

The initial – boundary value (IBVP) problem in nondimensional form becomes, for $J=c_{pw}\bar{J}/\varepsilon$,

$$\Theta_\eta-\Theta_{\xi\xi}+D_1U_{\xi\eta}=0\,,\ \text{in}\ (0,\infty)\times(0,J)\,, \tag{8}$$

$$U_{\eta\eta}-\lambda_A^2U_{\xi\xi\eta\eta}-\left(U_\xi-\lambda_B^2U_{\xi\xi\xi}-D_2\Theta\right)_\xi=0\,,\ \text{in}\ (0,\infty)\times(0,J)\,, \tag{9}$$

where $\lambda_A=\varepsilon^{-1}H/\sqrt{3}$, $\lambda_B=\varepsilon^{-1}g$, $D_1=\dfrac{a(3\lambda+2\mu)}{\rho c_e}$, $D_2=\dfrac{T_o a(3\lambda+2\mu)}{\rho c_w^2}$.

The boundary conditions for zero tractions at $\xi=0$ become

$$U_{\xi\xi}=0\ \text{ and }\ \lambda_A^2U_{\xi\eta\eta}+U_\xi-\lambda_B^2U_{\xi\xi\xi}-D_2\Theta=0\,, \tag{10}$$

while convection boundary condition (4) takes the form

$$\Theta_\xi=\mathrm{Bi}\left(\Theta-\Theta_\infty\right), \tag{11}$$

where $\mathrm{Bi} = \varepsilon C_c / k$ is the nondimensional Biot number characterizing the magnitude of convective heat transfer with respect to that of heat conduction. Note that for $\mathrm{Bi} \to \infty$ the free surface of the half space attains the temperature Θ_∞ and Robin condition (11) becomes $\Theta(\xi = 0, \eta) = \Theta_\infty(\eta)$. Again, for $\xi \to \infty$ zero displacement, displacement gradient and temperature are assumed. Finally, initial conditions (6) now read

$$U(x, t = 0) = U_\eta(x, t = 0) = \Theta(x, t = 0) = 0 \,. \tag{12}$$

The respective weakly coupled problem is derived upon setting $D_1 = 0$ in equation (8) thus eliminating the coupling term $U_{\xi\eta}$.

3 VARIATIONAL FORMULATION AND STABILITY OF THE WEAK SOLUTION

In this section, the variational formulation of IBVP (8)-(12) will be derived and subsequently studied with respect to the stability of the weak solution.

3.1 Variational Formulation

A proper setting for the variational formulation contitute the classical Sobolev (Hilbert) spaces $W^{k,p=2}(\Omega) \equiv H^k(\Omega)$, $k \in \mathbb{N}$ defined over a domain Ω. It is $H^0(\Omega) \equiv L^2(\Omega)$. We denote $\|\cdot\|_{H^k(\Omega)}, |\cdot|_{H^k(\Omega)}$ the induced norm and semi-norm resectively and $H^k(\Omega)^*$ the dual space of $H^k(\Omega)$. Finally we introduce the Banach value spaces $L^2(0, J; H^k(\Omega))$ with norm $\|\cdot\|^2_{L^2(0,J;H^k(\Omega))} = \int_0^J \|\cdot\|^2_{H^k(\Omega)} d\eta$.

Multiply equations (8), (9) with $\vartheta \in H^1(0, \infty)$, $v \in H^2(0, \infty)$ respectively. Integration by parts and use of boundary conditions (10) and (11), along with conditions at infinity, yields the variational problem: Find Θ, U such that

$$\int_0^\infty \vartheta \Theta_\eta d\xi + \int_0^\infty \vartheta_\xi \Theta_\xi d\xi + \mathrm{Bi}\,\vartheta(0)\Theta(0) + D_1 \int_0^\infty \vartheta U_{\xi\eta} d\xi = \mathrm{Bi}\,\vartheta(0)\Phi f(\eta) \,, \tag{13}$$

a.e. in $(0, J)$, for every $\vartheta \in H^1(0, \infty)$ and

$$\int_0^\infty v U_{\eta\eta} d\xi + \lambda_A^2 \int_0^\infty v_\xi U_{\xi\eta\eta} d\xi + \int_0^\infty v_\xi U_\xi d\xi + \lambda_B^2 \int_0^\infty v_{\xi\xi} U_{\xi\xi} d\xi - D_2 \int_0^\infty v_\xi \Theta d\xi = 0 \,, \tag{14}$$

a.e. in $(0, J)$, for every $v \in H^2(0, \infty)$.

3.2 Stability Estimate for the Weak Solution

The two following lemmas will be used in order to obtain a stability result for the above variational problem

Lemma 1 (Modified Young's Inequality) *Let* $\alpha, \beta \geq 0$, $1 < p < \infty$ *and* q *be the conjugate of* p, *i.e.* $p^{-1} + q^{-1} = 1$. *Then, for every* $\varepsilon \in \mathbb{R}_+$ *it is* $\alpha\beta \leq \varepsilon p^{-1} \alpha^p + \varepsilon^{-1} q^{-1} \beta^q$.

Lemma 2 (Gronwall) *Let* $u(t), g(t)$ *be continuous real functions with* $u(t) \geq 0$ *and* $c, J \in \mathbb{R}_+$. *Assume that*

$$u(t) \leq g(t) + c \int_0^t u(s) ds \,, \ \forall t \in [0, J] \,.$$

Then it is $u(t) \leq e^{ct} g(t)$, $\forall t \in [0, J]$.

We are now in position to prove the following result

Theorem *Assume that the solution of variational problem () satisfies* $U \in L^2(0,J;H^2(0,\infty))$, $U_\eta \in L^2(0,J;H^1(0,\infty))$, $U_{\eta\eta} \in L^2(0,J;L^2(0,\infty))$ *and* $\Theta \in L^2(0,J;H^1(0,\infty))$. *Then it is*

$$\left\|U_\eta\right\|_{L^2(0,J;H^1(0,\infty))} + \left\|U\right\|_{L^2(0,J;H^2(0,\infty))} + \left\|\Theta\right\|_{L^2(0,J;L^2(0,\infty))} \leq \frac{\mathrm{Bi}\Phi\sqrt{3\omega}}{c} J\sqrt{e^{\max(1,\omega,c^{-2})J}}\left\|\delta\right\|_{H^1(0,\infty)^*}, \tag{15}$$

where $\omega = D_2 / D_1$ *and* $c = \min(1,\lambda_A^2,\lambda_B^2,\omega)$.

Proof Set $\vartheta = \Theta$ in (13) and $v = U_\eta$ in (14). Multiply equation (13) by $D_2 / D_1 = \omega$ add (13) to (14) and note the resulting mutual cancelation of the coupling terms

$$D_1\int_0^\infty \vartheta U_{\xi\eta} d\xi \text{ and } -D_2\int_0^\infty v_\xi \Theta d\xi . \tag{16}$$

The final equation reads

$$\begin{aligned}&\int_0^\infty U_\eta U_{\eta\eta} d\xi + \lambda_A^2\int_0^\infty U_{\xi\eta}U_{\xi\eta\eta} d\xi + \int_0^\infty U_{\xi\eta}U_\xi d\xi + \lambda_B^2\int_0^\infty U_{\xi\xi\eta}U_{\xi\xi} d\xi \\ &\quad + \omega\int_0^\infty \Theta\Theta_\eta d\xi + \omega\int_0^\infty \Theta_\xi\Theta_\xi d\xi + \mathrm{Bi}\omega\Theta(0)^2 = \mathrm{Bi}\omega\Phi f(\eta)\left\langle\Theta,\delta(\xi)\right\rangle\end{aligned}, \tag{17}$$

where $\left\langle\cdot,\cdot\right\rangle$ denotes the pairing between $H^1(0,\infty)$ and its dual space $H^1(0,\infty)^*$. In fact, as will be shown later, the Dirac function $\delta(\xi)$ is smoother than required for the duality pairing to make sense in this 1D setting. Adding the term $\int_0^\infty U_\eta U d\xi$ to both sides of eq. (17), we may write

$$\begin{aligned}&\frac{d}{ds}\left\|U_s\right\|^2_{L^2(0,\infty)} + \lambda_A^2\frac{d}{ds}\left|U_s\right|^2_{H^1(0,\infty)} + \frac{d}{ds}\left[\left\|U\right\|^2_{L^2(0,\infty)} + \left|U\right|^2_{H^1(0,\infty)} + \lambda_B^2\left|U\right|^2_{H^2(0,\infty)}\right] \\ &+\omega\frac{d}{ds}\left\|\Theta\right\|^2_{L^2(0,\infty)} \leq \\ &\left|2\mathrm{Bi}\omega\Phi f(\eta)\right|\left|\left\langle\Theta,\delta(\xi)\right\rangle\right| - \omega\left|\Theta\right|^2_{H^1(0,\infty)} + 2\int_0^\infty U_s U d\xi \leq \\ &\left|2\mathrm{Bi}\omega\Phi\right|\left|\left\langle\Theta,\delta(\xi)\right\rangle\right| - \omega\left|\Theta\right|^2_{H^1(0,\infty)} + 2\int_0^\infty U_s U d\xi\end{aligned}, \tag{18}$$

since $\left|f\right| \leq 1$. Integrating with respect to time from $s = 0$, to $s = \eta \leq J$, leads to

$$\begin{aligned}&c\left(\left\|U_\eta\right\|^2_{H^1(0,\infty)} + \left\|U\right\|^2_{H^2(0,\infty)} + \left\|\Theta\right\|^2_{L^2(0,\infty)}\right) \\ &\qquad \leq 2\omega\mathrm{Bi}\Phi\int_0^\eta \left|\left\langle\Theta,\delta(\xi)\right\rangle\right| ds - \omega\int_0^\eta \left|\Theta\right|^2_{H^1(0,\infty)} ds + 2\int_0^\eta\int_0^\infty U_s U d\xi ds\end{aligned}, \tag{19}$$

where $c = \min(1,\lambda_A^2,\lambda_B^2,\omega)$. Applying the Cauchy-Schwarz inequality and Young's inequality with $p = q = 2$ and $\varepsilon = 1/c$, the second integral of the r.h.s. of (19), may be bounded as

$$2\int_0^\eta\int_0^\infty U_s U d\xi ds \leq \int_0^\eta \left(c\left\|U_s\right\|^2_{L^2(0,\infty)} + c^{-1}\left\|U\right\|^2_{L^2(0,\infty)}\right) ds . \tag{20}$$

The remaining integral may be handled as follows: First observe that $\delta(\xi) \in H^{-1/2-\gamma}(0,\infty) \subset H^1(0,\infty)^*$, $0 < \gamma \ll 1$. Using again the Cauchy-Schwarz inequality and Young's inequality with $p = q = 2$ and

$\varepsilon = \mathrm{Bi}\Phi / c$

$$\int_0^\eta \left|\left\langle \Theta, \delta(\xi)\right\rangle\right| ds \le \frac{c}{2\mathrm{Bi}\Phi}\int_0^\eta \left\|\Theta\right\|^2_{H^1(0,\infty)} ds + \frac{\mathrm{Bi}\Phi}{2c}\int_0^\eta \left\|\delta\right\|^2_{H^1(0,\infty)^*} ds\,. \tag{21}$$

Invoking (20) and (21), inequality (19) becomes

$$\begin{aligned}\left\|U_\eta\right\|^2_{H^1(0,\infty)} + \left\|U\right\|^2_{H^2(0,\infty)} + \left\|\Theta\right\|^2_{L^2(0,\infty)} \le \frac{\omega \mathrm{Bi}^2\Phi^2}{c^2}\int_0^\eta \left\|\delta\right\|^2_{H^1(0,\infty)^*} ds + \omega\int_0^\eta \left\|\Theta\right\|^2_{H^1(0,\infty)} ds \\ - \omega\int_0^\eta \left|\Theta\right|^2_{H^1(0,\infty)} ds + \max(1,\mathrm{c}^{-2})\left(\int_0^\eta \left\|U_s\right\|^2_{L^2(0,\infty)} ds + \int_0^\eta \left\|U\right\|^2_{L^2(0,\infty)} ds\right)\end{aligned}\,. \tag{22}$$

By definition it is $\left\|\Theta\right\|^2_{H^1(0,\infty)} = \left\|\Theta\right\|^2_{L^2(0,\infty)} + \left|\Theta\right|^2_{H^1(0,\infty)}$ and inequality (22) becomes

$$\begin{aligned}\left\|U_\eta\right\|^2_{H^1(0,\infty)} + \left\|U\right\|^2_{H^2(0,\infty)} + \left\|\Theta\right\|^2_{L^2(0,\infty)} \le \frac{\omega \mathrm{Bi}^2\Phi^2}{c^2}\int_0^\eta \left\|\delta\right\|^2_{H^1(0,\infty)^*} ds + \omega\int_0^\eta \left\|\Theta\right\|^2_{L^2(0,\infty)} ds \\ + \max(1,\mathrm{c}^{-2})\left(\int_0^\eta \left\|U_s\right\|^2_{L^2(0,\infty)} ds + \int_0^\eta \left\|U\right\|^2_{L^2(0,\infty)} ds\right)\end{aligned}\,. \tag{23}$$

Applying Gronwall's lemma, we get

$$\left\|U_\eta\right\|^2_{H^1(0,\infty)} + \left\|U\right\|^2_{H^2(0,\infty)} + \left\|\Theta\right\|^2_{L^2(0,\infty)} \le \frac{\omega \mathrm{Bi}^2\Phi^2}{c^2} J \left\|\delta\right\|^2_{H^1(0,\infty)^*} e^{\max(1,\omega,c^{-2})J}\,. \tag{24}$$

Integrating again with respect to time and using the Banach valued space norm definitions

$$\left\|U_\eta\right\|^2_{L^2(0,J;H^1(0,\infty))} + \left\|U\right\|^2_{L^2(0,J;H^2(0,\infty))} + \left\|\Theta\right\|^2_{L^2(0,J;L^2(0,\infty))} \le \frac{\omega \mathrm{Bi}^2\Phi^2}{c^2} J^2 \left\|\delta\right\|^2_{H^1(0,\infty)^*} e^{\max(1,\omega,c^{-2})J}\,. \tag{25}$$

Taking square roots and using the norm equivalence in $\mathbb{R}^3$, (25) yields (15). □

4 SEMI-DISCRETIZATION WITH FINITE ELEMENTS

Let us know introduce appropriate finite element spaces for conforming discetization of the variational problem under consideration. A first step is the approximation of the infinite domain $(0,\infty)$ with a finite one $(0, L(J))$, where the end point is selected such that conditions at infinity hold approximately in $L(J)$ for $\eta < J$, in the sense that there exists $\sigma \gg 0$ such that all the previously defined norms of the solution are smaller than $L(J)^{-\sigma}$ for $\eta \in (0, J]$ (for such an example in classical thermoelasticity see [11]). For the approximation of the temperature field we select $V^h_\Theta \subset H^1(0,L)$, such that for each $\bar{t} \in (0,T]$, fixed, it is $\Theta^h(\bar{t}) \in V^h_\Theta$. Similarly, for the approximation of the displacement field we have $U^h \in V^h_U \subset H^2(0,L)$. The discretized variational problem becomes: Find Θ^h, U^h such that

$$\int_0^L \vartheta^h \Theta^h_\eta d\xi + \int_0^L \vartheta^h_\xi \Theta^h_\xi d\xi + m\vartheta^h(0)\Theta^h(0) + D_1\int_0^L \vartheta^h U^h_{\xi\eta} d\xi = \vartheta^h m\Phi H(\eta)\delta(\xi)\,, \tag{26}$$

a.e. in $(0, J)$ for every $\vartheta^h \in V^h_\Theta$ and

$$\int_0^L v^h U^h_{\eta\eta} d\xi + \lambda_A^2\int_0^L v^h_\xi U^h_{\xi\eta\eta} d\xi + \int_0^L v^h_\xi U^h_\xi d\xi + \lambda_B^2\int_0^L v^h_{\xi\xi} U^h_{\xi\xi} d\xi - D_2\int_0^L v^h_\xi \Theta^h d\xi = 0\,, \tag{27}$$

a.e. in $(0, J)$ for every $v^h \in V^h_U$.

For the approximation of the temperature field quadratic Lagrange interpolation polynomials are selected, while the displacement field is approximated with Hermite polynomials of degree 5. The definition of approximation spaces V_Θ^h and V_U^h is

$$V_\Theta^h = \left\{ w^h \in H^1(0,L) : w^h\big|_e = \sum_{i=1}^{6} L_i(x) w_i^h(t) \right\},\ V_U^h = \left\{ w^h \in H^2(0,L) : w^h\big|_e = \sum_{i=1}^{6} H_i(x) w_i^h(t) \right\}, \quad (28)$$

where $L_i, i=1,2,3$ and $H_i, i=1,2,..,6$ denote the corresponding Lagrange and Hermite shape functions (see also Figure 3) and w_i^h are the approximate nodal values for Θ in (28) and U, U_x in (29) respectively.

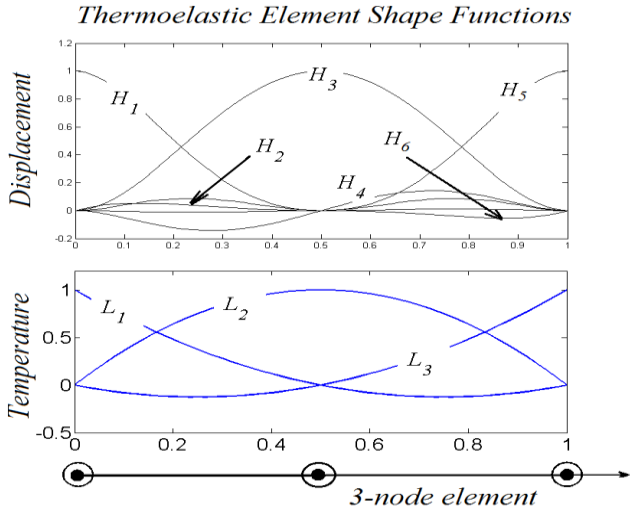

Figure 3. Thermoelastic element shape functions.

Time integration of the resulting, from the spatial discretization with finite elements, ordinary differential system is performed, after the second order system is transformed to an equivalent first order one, with the Crank-Nicolson method.

5 RESULTS AND DISCUSSION

The problem of thermal shock response for the gradient elastic half-space is solved for two different values of the Biot Number. In particular, the cases $\mathrm{Bi}=1$ and $\mathrm{Bi}=\infty$ are considered. The second case corresponds to the application of a Dirichlet condition on the upper surface of the half space, such that the temperature at this point attains the value Θ_∞ immediately at time $\eta = 0$ (see also section 2.2). In all cases we set $f = H(\eta - 0)$. The material properties selected are typical for ceramic refractories ($k = 33W/mK$, $\rho = 4000kg$, $c_e = 755J/kgK$, $a = 4.6e-6K^{-1}$, $E = 416e9N/m^2$, $\nu = 0.23$).The solution is obtained for both the fully and weakly coupled systems. A sequence of finite element meshes is considered. The number of finite elements N_{el} employed for the solution is increased as $N_{el} = 100, 200, 400, 800, 1600$. In all cases we select the number of time steps N_t to be twice the number of the elements ($N_t = 2N_{el}$). Convergence characteristics of the proposed finite element method are plotted in Figure 4 for different values of the microstructural parameters. As an error indicator we select the quantity

$$e_{N_{el}} = \frac{\max\limits_{x\in[0,L],t\in[0,J]} \left| solution(N_{el}=3200) - solution(N_{el}) \right|}{\max\limits_{x\in[0,L],t\in[0,J]} \left| solution(N_{el}=3200) \right|}. \quad (29)$$

Both scales in Figure 4 are logarithmic. Observe that the convergence of the displacement field FE solution (blue line) is more rapid that of the temperature field (red line). This is attributed to the higher order approximation

used for the displacements. In all cases the relative error for the displacement is less than 1%. Finally the error values are almost identical for the fully coupled and weakly coupled system.

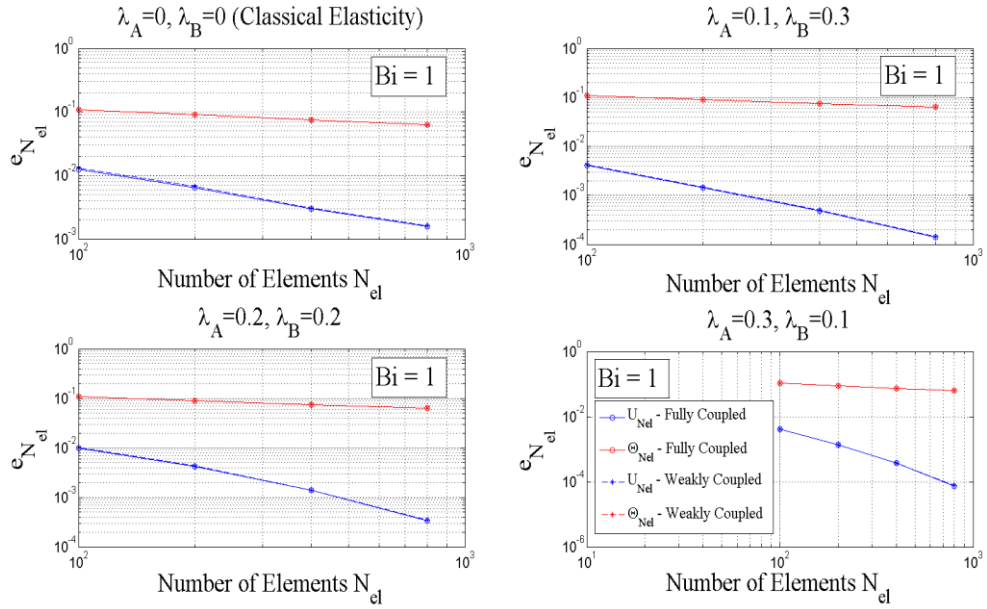

Figure 4. Convergence of the finite element solution for the temperature (red line) and displacement (blue line) field. The convergence lines, as functions of the Number of elements are plotted in logarithmic scales.

Figures 5 and 6 are plots of the displacement solution for $\mathrm{Bi}=1$ and $\mathrm{Bi}=\infty$ respectively. In both cases three different combinations of the microstructural parameters are selected. The displacement field is plotted as a function of the spatial parameter at three time instances ($\eta=5,10,20$). The classical elasticity solution ($\lambda_A=\lambda_B=0$) is also plotted. Comparing Figures 5 and 6 it is observed that the solution is smoother and of lower amplitude for small value of the Biot number. The dispersive nature of pulses characterizing gradient elasticity solutions is evident for the cases where the microstructural parameters are dissimilar. The case ($\lambda_A=\lambda_B=0.2$) shows almost zero dispersion. This is in accordance with the dispersion analysis of gradient elastic solutions [1], [12].

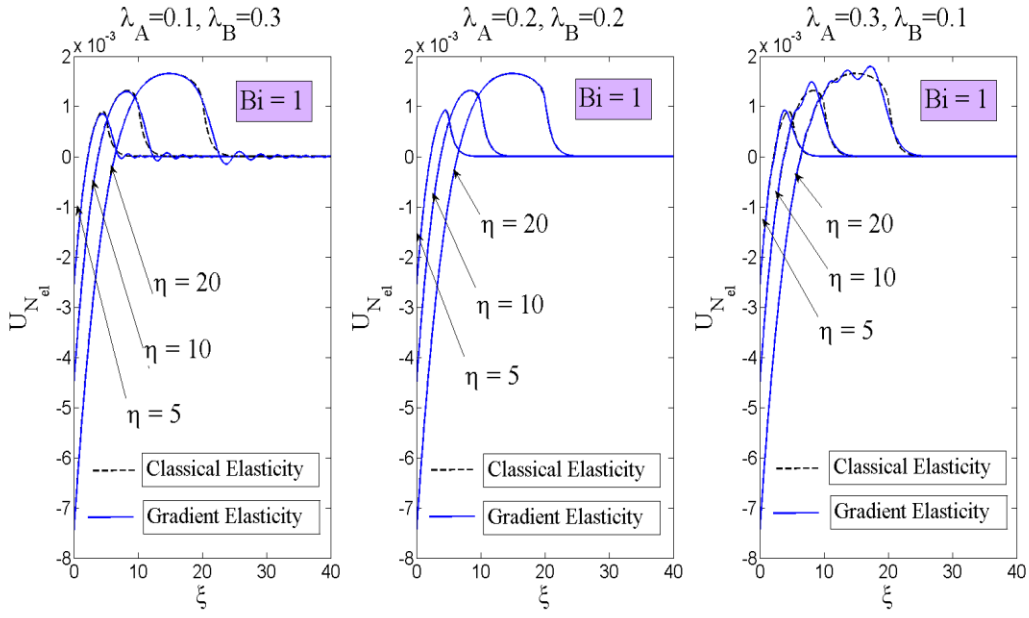

Figure 5. Displacement field at different time instances, for selected values of the microstructural parameters λ_A, λ_B and $\mathrm{Bi}=1$. Finite element solution for $N_{el}=1600$ and $N_t=3200$. The classical elasticity solution is also displayed as reference.

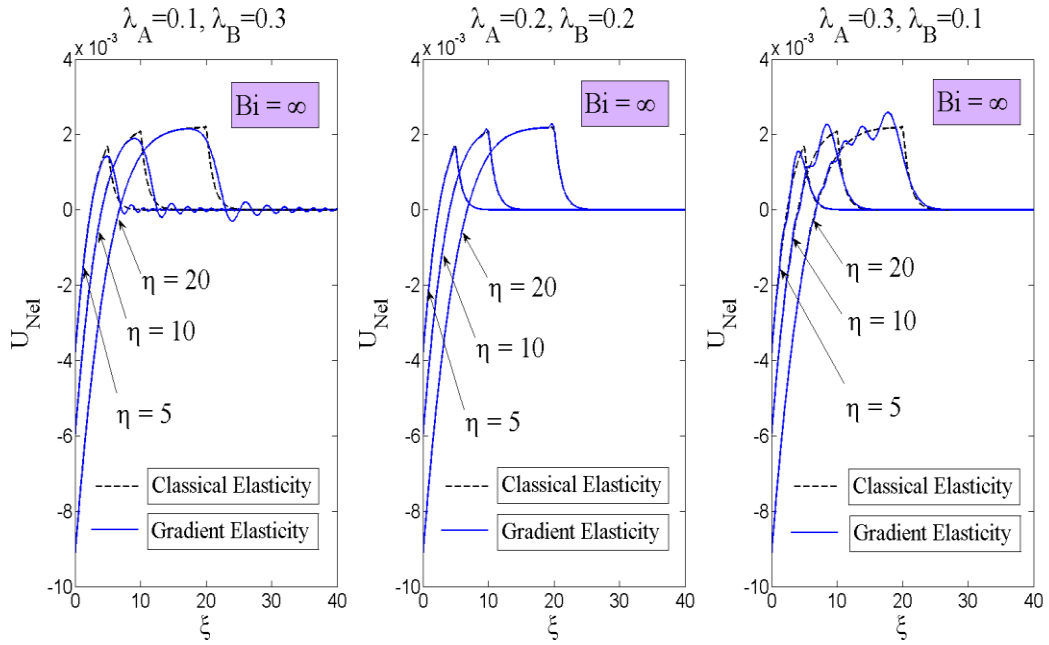

Figure 6. Displacement field at different time instances, for selected values of the microstructural parameters λ_A, λ_B and $\mathrm{Bi}=\infty$. Finite element solution for $N_{el}=1600$ and $N_t=3200$. The classical elasticity solution is also displayed as reference.

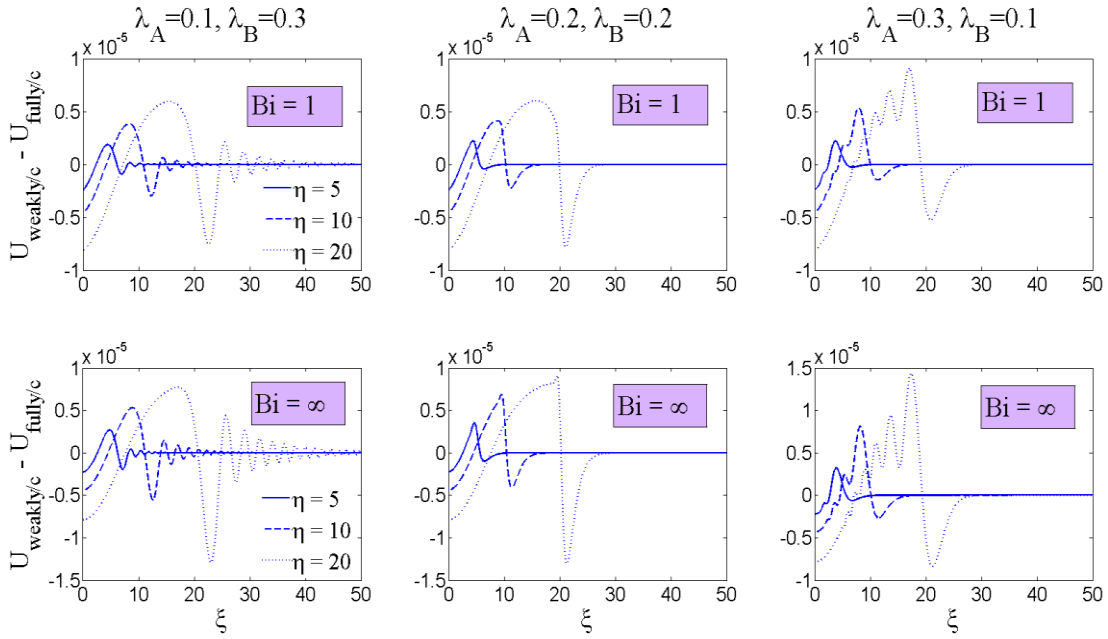

Figure 7. Displacement field solution difference between the fully and weakly coupled system. The difference is plotted for time instances corresponding to those plotted in figures 5 and 6.

Figure 7 is a plot of the difference between the solutions of the fully and weakly coupled system. The difference is two orders of magnitudes smaller than the actual solution and thus the fully coupled and weakly coupled systems yield almost identical results for the ceramic (refractory) material selected.

For the weakly coupled system, we may derive an energy balance equation by testing the variational form (14), after setting $D_1=0$ in (13), with $v=U_\eta$. The energy balance equation reads

$$E(\eta)=\left\|U_\eta\right\|^2_{L^2(0,\infty)}+\lambda_A^2\left|U_\eta\right|^2_{H^1(0,\infty)}+\left|U\right|^2_{H^1(0,\infty)}+\lambda_B^2\left|U\right|^2_{H^2(0,\infty)}=2D_2\int_0^\eta\int_0^\infty U_{\xi s}\Theta d\xi ds=2P(\eta)\,, \quad (30)$$

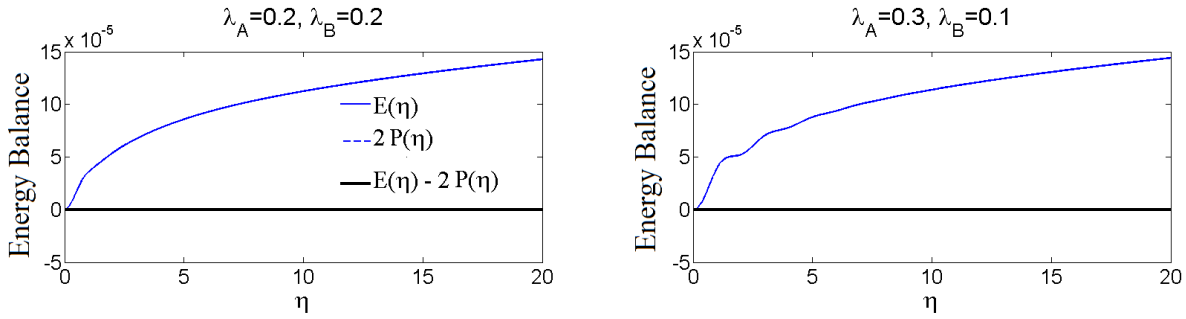

Figure 8. Energy balance for the solution of the weakly couled system. Two different sets of microstructural parameters are considered.

The temperatura solution Θ is this case is the solution of the heat equation in the half space. Figure 8 shows the energy balance equation (30) that is verified by the FE solution of the weakly coupled system.

6 CONCLUSIONS

The thermoelastic response of a gradient elastic half-space, subjected to thermal shock on its free boundary has been studied by means of the Finite Element method. Thermal shock is imposed through a Robin boundary condition expressing convection heat transfer with a fluid medium. The gradient thermoelastic pulses are of dispersive nature and smoother than those obtained from classical thermoelasticity. Finally for the material selected (ceramic) the differences between the solutions of the fully and weakly coupled theroelastic models are found to be negligible. The convergence of the FE scheme is established through a large number of numerical experiments and the scheme is found to be robust, yielding small error values for relatively coarse meshes.

Acknowledgement: Support from the European Union FP7 project "*Mechanics of refractory materials at high–temperature for advanced industrial technologies*" under contract number PIAPP–GA–2013–609758 is gratefully acknowledged.

REFERENCES

[1]. Mindlin, R.D. (1964), "Micro-structure in Linear Elasticity", *Arch. Rat. Mech. Anal*., Vol. 16, pp. 51-78.
[2]. Danilovskaya, V.I. (1952), "On a dynamic problem of thermoelasticity", *Prikl. Math. Mech*., Vol.16, No. 3.
[3]. Danilovskaya, V.I. (1950), "Thermal stresses in an elastic half-space arising after a sudden heating of its boundary", *Prikl. Math. Mech*., Vol.14, No. 3.
[4]. Hetnarski, R.B., Eslami, M.R. (2009), *Thermal Stresses – Advanced Theory and Applications*, Springer, Berlin.
[5]. Kovalenko, A.D. (1969), *Thermoelasticity. Basic Theory and Applications*, Wolters-Noordhoff Publishing, Groningen, the Netherlands.
[6]. Nowacki, W. (1975), *Dynamic Problems of Thermoelasticity*, Noordhoff Int. Publishing, Leyden, the Netherlands.
[7]. Quintanilla, R. (2003), "Thermoelasticity Without Energy Dossipation of Nonsimple Materials", *ZAMM*, Vol. 83, pp. 172-180.
[8]. Ieşan, D. (1989), "Thermoelasticity of Non-SimpleMaterials", *J. Therm. Stresses*, Vol. 12, pp. 545-557.
[9]. Filopoulos, S.P., Papathanasiou, T.K., Markolefas, S.I. and Tsamasphyros, G.J. (2014), "Generalized Thermoelastic Models for Linear Elastic Materials with Micro-Structure Part I: Enhanced Green-Lindsay Model", *J. Therm. Stresses*, Vol. 37(5), pp. 624-641.
[10]. Filopoulos, S.P., Papathanasiou, T.K., Markolefas, S.I. and Tsamasphyros, G.J. (2014), "Generalized Thermoelastic Models for Linear Elastic Materials with Micro-Structure Part II: Enhanced Lord-Shulman Model", *J. Therm. Stresses*, Vol. 37(5), pp. 642-659.
[11]. Jiang, S. (1990), "Numerical solution for the Cauchy problem in nonlinear 1D thermoelasticity", *Computing*, Vol. 44, pp. 147-158.
[12]. Filopoulos, S.P., Papathanasiou, T.K., Markolefas, S.I. and Tsamasphyros, G.J. (2010), "Dynamic Finite Element Analysis of a Gradient Elastic Bar with micro-inertia", *Comput. Mech*., Vol. 45, pp. 311-319.